George Gehring
Hideko Iwamoto
Doug Will

Analysis of the Feasibility of a Metal-Loaded Liquid Scintillator Detector for the MOON Project

The MOON (Molybdenum Observation Of Neutrinos) project is an experiment which intends to determine whether the neutrino is a Majorana particle or a Dirac particle. If the former is true, MOON also has the potential to determine the mass of the neutrino very accurately. It will accomplish this by trying to observe the $\beta\beta(0\nu)$ decay of ^{100}Molybdenym. The current design proposal for the MOON detector is a large 'foil sandwich' of thin sheets of molybdenum foil positioned between slabs of plastic scintillator, with fiber outputs to photomultiplier tubes (PMTs), or perhaps avalanche photodiodes (APDs). Another detector design being considered is a spherical molybdenum-loaded liquid-scintillation detector, similar in design to SNO.

Reduction of background radiations is an important consideration in either detector. The 26000 m^2 surface area of the plastic scintillator modules in the 'foil sandwich' must be kept dust-free so that unwanted background sources such as Rn and its daughters are avoided.[1] This would require extensive cleanroom facilities for production, transportation, and operation of the detector. On the other hand, liquids are very easily purified and can be conveniently reprocessed once the detector is constructed and in operation, making the liquid-scintillation detector an attractive option. The use of APDs in place of PMTs would also help reduce background radiation. APDs occupy much less volume than PMTs, resulting in less excess material around the detector to harbor background sources. Since Silicon is a very clean substrate, the glass and metals used in PMTs are more likely to contain radionuclides than an APD.

APDs have several other advantages when compared to PMTs. APDs have much higher quantum efficiencies, and when operated in the Geiger mode can be employed for single-photon counting, which would be the most accurate method for measuring the energy of an event. They are also lighter and require less rigorous support structures. APDs have lower operating voltages, are insensitive to magnetic fields, are less fragile than PMTs, and have long operating lifetimes. However, APDs are also susceptible to defects which can cause dark counts, afterpulsing, and optical crosstalk.[2]

The long half-life for ^{100}Mo $\beta\beta(0\nu)$ makes it imperative that large amounts of Mo are contained in the detector. The spherical design's maximum volume for minimum surface area relationship makes it an attractive shape for a detector, provided a high enough concentration of Mo in liquid scintillator can be achieved. A smaller surface area requires fewer APDs or PMTs, lowering the cost of the detector.

[1] Elliot S and Vogel P, Annu. Rev. Nucl. Part. Sci. **52** (2002)

[2] W.J. Kindt, Geiger Mode Avalanche Photodiode Arrays for spatially resolved single photon counting, **5**, Delft University Press, 1999.

A single-photon sensitive detector can be modeled over the region of interest by analytical equations. These give the researcher the ability to quickly modify detector parameters and re-evaluate detector effectiveness, a powerful tool in the development process. Furthermore, predictions of these analytical equations can be used to check the consistency of Monte Carlo results. Analytical equations are also helpful for developing a method for the reconstruction of an event from the resultant data patter (generated by Monte Carlo or by a prototype detector).

For the following derivation, the proposed situation is a spherical detector of radius R, which is completely covered (with no dead space) at the surface by M 'pixels', which for our discussion will be APDs (though the calculations are equally applicable for PMTs). Initially we will assume that each pixel is 100% efficient.

The first equation we need to develop is an expression for the photon flux at any point in the sphere of radius R from an arbitrary event location. We take a source event of N photons at point E, a distance r away from the center of the detector, as shown in Figure 1. The line $\overline{OE}$ is the event axis, from which all angles are measured. At a point S on the surface of the sphere a distance k away from the event source, the photon flux will be

$$\Phi = \frac{N}{4\pi k^2} \tag{1}$$

A straight line $\overline{ES}$ makes an angle α with the event axis, while the line $\overline{OS}$ makes an angle θ with the event axis. From the law of cosines, we can express k as a function of R, r, and θ:

$$k^2 = R^2 + r^2 - 2rR\cos\theta \tag{2}$$

We can also determine the following relationships between α and θ:

$$R\sin\theta = k\sin\alpha \tag{3}$$

$$R\cos\theta = r + k\cos\alpha \tag{4}$$

however, since the flux is perpendicular to $\overline{ES}$, and the surface of the sphere is not perpendicular to $\overline{ES}$, we need to include a scaling factor in our flux equation. A differential section of area dA' on the surface of a sphere with radius k centered at E will map to a section of area on the sphere of radius R, represented in Figure 2. If we say that the area mapped on the larger sphere is dA, we can express this relationship as

$$dA' = dA\cos\delta \tag{5}$$

where $\delta = \alpha - \theta$. The scaling factor should be $\frac{dA'}{dA} = \cos(\alpha - \theta)$, so our resultant flux equation looks like:

$$\Phi = \frac{N\cos(\alpha - \theta)}{4\pi k^2} \tag{6}$$

Using the trigonometric difference identity and using (3) and (4) to eliminate α, we have:

$$\Phi = \frac{N}{4\pi k^2}\left[\frac{R}{k}\cos^2\theta - \frac{r}{k}\cos\theta + \frac{R}{k}\sin^2\theta\right] = \frac{N(R - r\cos\theta)}{4\pi k^3} \tag{7}$$

And substituting with (2) to eliminate k:

$$\Phi(r, N, R) = \frac{N(R - r\cos\theta)}{4\pi(R^2 + r^2 - 2rR\cos\theta)^{\frac{3}{2}}} \tag{8}$$

which is an equation for photon flux at any point in the sphere as a function of the sphere's radius R, the displacement of the event from the center of the sphere r, the magnitude of the event in photons N, and the position of the point on the sphere as referenced by the angle θ it makes with the event axis. Note that the point on the sphere closest to E is always at $\theta = 0$, while the point farthest from E is always at $\theta = \pi$, excluding central events (where all distances would be equal).

Since photon detection is a statistical process, we must allow for the probability that multiple photons will hit a single detector pixel, resulting in the 'loss' of all photons but the first. We model this probability with a Poisson distribution based on the local photon flux. For a central event, the average photon flux at any point in the sphere is $\frac{N}{M}$, where M is the number of pixels in the detector. Thus, the Poisson probability distribution is expressed as:

$$P(\gamma) = \frac{\left(\frac{N}{M}\right)^{\gamma} e^{-\frac{N}{M}}}{\gamma!} \tag{9}$$

where γ is the integer number of photons detected by the particular pixel.

The probability that a pixel is hit is simply the sum of the probabilities for $\gamma > 0$, or

$$\sum_{\gamma=1}^{N} P(\gamma) = 1 - P(0). \tag{10}$$

This is from the perspective of a particular *pixel*, however. We wish to know the probability that a particular *photon* is detected or not detected (due to pileup). The probability that a photon is detected is equivalent to the probability that the pixel it is entering has not been hit by another photon. If we assume (as we have in the above calculation) that all photons hit simultaneously, the probability for detection for an arbitrary photon is $P(0)$, or $e^{-\frac{N}{M}}$ for a central event.

Next we want to take the event off-center, and allow it to happen at any point in the sphere. We need to define a local photon flux, $\frac{dN}{dM}$, which is the number of photons in a differential number of pixels dM which inhabit a small area dA. The number of photons passing through dA is simply ΦdA, while the number of pixels in dA is $\frac{dA}{D}$, where D is the area of an individual pixel. The

dA factors cancel, and we are left with the local photon flux as

$$\frac{dN}{dM} = \Phi D = \frac{ND(R - r\cos\theta)}{4\pi(R^2 + r^2 - 2rR\cos\theta)^{\frac{3}{2}}} \tag{11}$$

Since we're interested in $P(0)$, we simply exponentiate the opposite of this expression to get our new probability, which is now a function of R, D, r, and θ.

$$P_{detection}(r, R, D, \theta) = e^{-\frac{dN}{dM}} = e^{\left(-\frac{ND(R-r\cos\theta)}{4\pi(R^2+r^2-2rR\cos\theta)^{\frac{3}{2}}}\right)} \tag{12}$$

We're intending to put this probability into a binomial distribution later, so we have to make sure that it's acceptable for such a situation. R, D, and r are variables we will set for a specific scenario, but θ varies from 0 to π for any situation, so we need to eliminate it. We can take an average probability over the entire surface of the sphere by multiplying by the photon flux (number of photons at the point in question) and integrating with respect to θ and ϕ as follows:

$$< p > (r, N, D, R) = \frac{\int_0^{2\pi}\int_0^{\pi} P_{detection}(r, R, D, \theta)\Phi(r, N, R)R^2\sin\theta d\theta d\phi}{\int_0^{2\pi}\int_0^{\pi}\Phi(r, N, R)R^2\sin\theta d\theta d\phi} \tag{13}$$

We can substitute (8) and (12) into (13), integrate over $d\phi$, substitute $\frac{4\pi R^2}{M}$ for D, and cancel some terms to get

$$p(r, N, M, R) = \frac{\int_0^{\pi} \frac{e^{\left(\frac{-NR^2(R-r\cos(\theta))}{M(R^2+r^2-2rR\cos(\theta))^{\frac{3}{2}}}\right)}(R-r\cos(\theta))\sin(\theta)d\theta}{(R^2+r^2-2rR\cos(\theta))^{\frac{3}{2}}}}{\int_0^{\pi}\frac{(R-r\cos(\theta))\sin(\theta)d\theta}{(R^2+r^2-2rR\cos(\theta))^{\frac{3}{2}}}} \tag{14}$$

This can be evaluated for a set of values r, N, M, and R. Figure 3 is a plot of p vs. r for $N = 10^4$, $M = 10^6$.

The downfall of this method is that it assumes all of the photons are arriving at the same time. Viewing the process sequentially, the first photon emitted will have a detection probability equal to 1, because none of the pixels have been hit before it, thus all are 'free.' The second photon will have a detection probability of $\frac{M-1}{M}$. This is where the process becomes complicated, because the detection probability for the third photon is dependant on whether photon 2 is or is not detected (hits the same pixel as photon 1). If photon 2 is not detected, photon 3 has the same number of free pixels available to it, and thus the same probability for detection. However, if photon 2 is detected, then there is one fewer free pixel, and photon 3 has a detection probability of $\frac{M-2}{M}$. For the n^{th} photon, the probability ranges from $\frac{M-1}{M}$ to $\frac{M-(n-1)}{M}$. This branching nature can be more clearly seen in a matrix form. Below, this is expressed with Photon

Number as the vertical index:

$$\begin{array}{c} \\ 1 \\ 2 \\ 3 \\ 4 \\ 5 \\ 6 \\ \\ \end{array} \begin{array}{c} \begin{array}{ccccc} 0 & 1 & 2 & 3 & 4 \end{array} \\ \begin{pmatrix} 1 & 0 & 0 & 0 & 0 \\ \frac{M-1}{M} & 0 & 0 & 0 & 0 \\ \frac{M-2}{M} & \frac{M-1}{M} & 0 & 0 & 0 \\ \frac{M-3}{M} & \frac{M-2}{M} & \frac{M-1}{M} & 0 & 0 \\ \frac{M-4}{M} & \frac{M-3}{M} & \frac{M-2}{M} & \frac{M-1}{M} & 0 \\ \frac{M-5}{M} & \frac{M-4}{M} & \frac{M-3}{M} & \frac{M-2}{M} & \frac{M-1}{M} \\ \vdots & \vdots & \vdots & \vdots & \vdots \end{pmatrix} \end{array}$$

Each element of the above matrix represents the probability for the sequence to progress in a downward fashion in the matrix. The probability to progress one space to the right (diagonally down) is $q_{ij} = 1 - p_{ij}$. In this form, the number of 'missed' photons is given by the column index, as shown above the matrix. it is to be noted that the last photon has a minimum detection probability of $\frac{M-(N-1)}{M}$, which is approximately what the Poisson statistics developed above predict for a central event. Thus, we have reason to believe that the Poisson probability is too low.

An average probability could be found from the sequential method by evaluating a weighted sum over every element in the matrix. The weighting $w_{i,j}$ for any element is the sum of the products of the weighting and progression probability for the two elements directly leading to that element, $w_{(i-1),j}p_{(i-1),j} + w_{(i-1),(j-1)}q_{(i-1),(j-1)}$. Each weighting can then be backward-simplified in turn until the only weighting remaining is $w_{2,1}$, which is equal to 1. The resulting equation can be mathematically expressed as

$$w_{i,j} = \prod_{a=1}^{i-2} \sum_{k=j-a}^{j} p_{(i-a),k} \quad \text{for} \quad i < j \tag{15}$$

A less computationally demanding (though also less accurate) method of finding an average probability would be to sum only the first column of the matrix, as all of the elements of the other columns have at least 1 q (low probability) in their weightings. Unfortunately, this matrix method is not easily moved off-center. We could instead calculate the probabilities for each photon by substituting n for N in equation (14) and summing from $n = 0$ (for the first photon) to $n = N - 1$ (for the last photon). Figure 4 is a plot of $p(r, n, M, R)$ for $r = 0$, $M = 10^6$, and $R = 5$. As you can see, this is very linear at the values of n we're using (around 10^4). As a result, this sum is very well approximated by simply evaluating $p(r, \frac{N}{2}, M, R)$.

$$\sum_{n=0}^{N-1} p(r, n, M, R) \approx p(r, \frac{N}{2}, M, R) \tag{16}$$

Now that we have an expression for the probability of detection for a photon, we can construct a distribution to represent the probability that the detector

will register x hits for an event of magnitude N at any point a distance of r off-center in a detector with M pixels and radius R. The binomial distribution is appropriate on the entire range from 0 to N, and our distribution looks like this:

$$Pb(x, N, p) = \frac{N!}{x!(N-x)!} p^x (1-p)^{N-x} \tag{17}$$

This equation has a shortcoming however - it is limited to small values of N (for the purpose of plotting with a computer program such as Maple or Mathematica) due to the factorials in the coefficient. For plotting with a computer, we need an equation which can be evaluated more easily. Using Stirling's formula, $\ln(N!) = N\ln(N) - N + \frac{1}{2}\ln(2\pi N)$, we can simplify the coefficient to:

$$\ln\left(\frac{N!}{x!(N-x)!}\right) = N\ln\left(\frac{N}{N-x}\right) + x\ln\left(\frac{N-x}{x}\right) + \frac{1}{2}\ln\left(\frac{N}{2\pi x(N-x)}\right) \tag{18}$$

and the other two terms are simply $x\ln(p)$ and $(N-x)\ln(1-p)$ respectively.

The new distribution is just the exponentiated sum of the above terms, thus our approximation looks like:

$$Pb_{approx} = e^{\left(N\ln\left(\frac{N}{N-x}\right) + x\ln\left(\frac{N-x}{x}\right) + \frac{1}{2}\ln\left(\frac{N}{2\pi x(N-x)}\right) + x\ln(p) + (N-x)\ln(1-p)\right)}$$

This approximation is very good for most values of x, but breaks down when x or $(N-x)$ is small because Stirling's formula is not valid. However, for small x or $(N-x)$, most of the factors of $N!$ will cancel with factors of the $(N-x)!$ or $x!$ in the denominator, leaving only a few multiplications that are easily done by a computer. We can express this simplified form of the binomial distributions as:

$$\left(\prod_{k=0}^{x-1}(N-k)\right)\frac{p^x(1-p)^{N-x}}{x!} \text{ for small } x \tag{20}$$

$$\left(\prod_{k=0}^{N-x-1}(N-k)\right)\frac{p^x(1-p)^{N-x}}{(N-x)!} \text{ for small } N-x \tag{21}$$

For $N > 10^3$, the approximation derived using Stirling's formula begins to deviate significantly at 2 units from the edge of the distribution (i.e. $x < 2$, $N - x < 2$). Thus, to be safe, we use the simplified binomial distribution for $x < 3$ and $N - 3 < x$ and use the approximation on the rest of the range, resulting in a piecewise function:

$$Prob(x, N, p) = \left\{ \begin{array}{cc} \left(\prod_{k=0}^{x-1}(N-k)\right)\frac{p^x(1-p)^{N-x}}{x!} & x < 3 \\ Pb_{approx} \text{ (equation 19)} & 3 < x < N-3 \\ \left(\prod_{k=0}^{N-x-1}(N-k)\right)\frac{p^x(1-p)^{N-x}}{(N-x)!} & N-3 < x \end{array} \right\} \tag{4}$$

This distribution represents the probability for a particular number of hits per event. Now that we have an expression for this distribution, it is a simple

exercise on the computer to find the centroid and line width (standard deviation).

Since we are interested in the actual energy of the event, we need to relate the mean number of hits $\overline{x}$ to a direct measure of the energy, such as N. The mean number of hits should just be the number of source photons multiplied by the probability of detection for an arbitrary photon:

$$\overline{x} = Np \tag{23}$$

where p is equation (14) evaluated as shown in equation (16). We can use this expression to translate mean number of hits into number of source photons (since $p(0)$ is dependant on N). Figure 5 is a plot of $\overline{x}$ vs. N for $M = 10^6$ and $r = 0$.

The energy resolution (standard deviation) can be obtained by computing the standard deviation of the distribution given by equation (22), and dividing by a factor that relates number of hits to number of photons for a particular value of N. The slope of equation (23) at any point represents this relationship, so the differential coefficient $\alpha = \frac{d}{dN}(\overline{x})$ evaluated at N is the factor we should use. Using the product rule, we see that

$$\alpha = p + N\frac{dp}{dN}$$

The exponential in the probability integral p is the only factor in the differential that depends on N, so the differentiation $\frac{dp}{dN}$ is easily carried out:

$$\alpha(p, N, R, r, M) = p - N\frac{\int_0^\pi \frac{e^{\left(\frac{-NR^2(R-r\cos(\theta))}{M(R^2+r^2-2rR\cos(\theta))^{\frac{3}{2}}}\right)} R^2(R-r\cos(\theta))^2\sin(\theta)d\theta}{M(R^2+r^2-2rR\cos(\theta))^3}}{\int_0^\pi \frac{(R-r\cos(\theta))\sin(\theta)d\theta}{(R^2+r^2-2rR\cos(\theta))^{\frac{3}{2}}}} \tag{24}$$

where p is again equation (14) evaluated as in (16). This is another equation which is difficult to graph, but can be evaluated for a given N, M, R, and r. α is nearly 1 for $N << M$, and approaches 0 as N approaches and exceeds M. Since α is in units of $\frac{\text{hits}}{\text{photons}}$, we divide the standard deviation of our hit distribution by α to calculate the energy resolution for an event fitting the provided conditions. Figure 6 is a plot of Energy Resolution vs. Position of Event (r) for $N = 10^4$, $M = 10^6$, and $R = 5$, and assuming a 3 MeV event energy. This corresponds to about 0.07% energy resolution at the center of the sphere, and 1% near the outside edge.

The previous calculation assumes that there are exactly N photons per event, which is not realistic. To correct for this, we can convolve our function with a distribution function for the source; for our purposes we choose to use a Guassian function g centered at 0 (so we don't disrupt the position of the centroid) and $\sigma = \sqrt{N}$. Thus, for some N and p, we have:

$$\int_0^\infty Prob(v, N, p)g(x - v)dv. \tag{25}$$

Unfortunately, the distribution $Prob(x, N, p)$ is not easily convolved with anything analytically or numerically by computer. However, since the function is based on a binomial distribution, we can model it very effectively with a Gaussian as well, with a mean and standard deviation equal to that of $Prob(x, N, p)$. Figure 7 shows the probability distribution $Prob(x, N, p)$ and the Gaussian approximation on the same graph, and Figure 8 shows the resultant Energy Resolution vs. Position of Event graph for the $M = 10^6$ and $R = 5$. The energy resolution has expanded to about 1% at the center of the sphere, reaching just over 2% at the edge.

Reconstructing the location of an event is also critical in a liquid-scintillation detector, because the amount of molybdenum (and thus the fiducial volume) must be known precisely. The hit pattern relative to the event axis should closely resemble the photon flux distribution given by equation (8). The event axis must be known for this to be useful; luckily there are several methods for accomplishing this. If a position vector is assigned to every pixel on the sphere (with magnitude R), one can treat a hit pixel as a point mass, and a vector sum of the hit pixels (effectively finding the 'center of mass' of the 'mass distribution') would result in a vector pointing in the direction of the event axis. Another possible method would be to find the areas on the sphere which have the greatest and smallest density of hit pixels, and use the points of greatest and least density to construct an axis.

Once the axis is known, a graph of Photon Density vs. θ can be created, and the distribution can be compared to those generated by equation (8) (See Figure 9). The most straightforward method for this is modeling the data with a Gaussian and comparing line width to predicted values, possibly via a graph of Line Width vs. r developed from equation (8). the background due to dark counts should be fairly isotropic, and on a graph of Hit Density vs. θ (resembling Figure 9) will manifest itself as a constant distribution. The distribution due to the distance off-center of the event location will be superimposed on this constant background distribution. If the background rate is known the constant background distribution could be subtracted out.

The above discussion considers an ideal situation. In reality, the quantum efficiency of the detectors will be less than 100% (and lower still if PMTs are used), and there will be dead space in the detector (again, more with PMTs). Both the efficiency and the dead space should manifest themselves as constant factors ϵ and η in the probability expression given in equation (14). These omissions are not the only problems with this detector design, however.

Avalanche photodiodes operated in Geiger mode at room temperature have a large dark count rate. For a device with an active area of 0.2 mm^2, the dark count rate can exceed 15,000 cps at room temperature.[3] If we assume that the dark count rate scales linearly with area, that's over 7x10^6 counts per second for a 10mm x 10mm square detector, of which approximately 10^6 would be needed to cover a detector of $R = 5$m. Over an approximate event period of 200ns, each detector would fire 1.5 times due to noise alone. Seeing a 10,000 photon event

[3]PerkinElmer Optoelectronics, available at http://opto.perkinelmer.com/Downloads/c30902e.pdf

on top of a background signal 150 times larger is a tall order for any detector.

One option is to cool the detector. At -25^{O}C, the dark count rate drops to 350 cps for a 0.2 mm^2 device.[4] Using the same scaling as above, each 100mm^2 detector would fire 0.036 times per event, resulting in 36,000 dark counts per event. This dark count rate is more reasonable, but still not desireable. Further cooling would reduce the background signal to more acceptable levels. If the relationship between dark count rate and temperature is linear, dropping to -50^{O}C would reduce the dark count rate to a very manageable 1,800 counts per event.

Cost is also a hurdle that needs to be overcome before this detector is feasible. A single avalanche photodiode can cost around $400, making the cost of detectors alone around $400 million dollars (before bulk pricing). Bulk discounts may apply, which would soften this number somewhat, as would using enriched molybdenum or dissolving a higher concentration of molybdenum in the liquid scintillator. Unfortunately, dissolving molybdenum in liquid scintillator is not a trivial task. It is highly colored in many solutions, and some of the clear molybdenum solutions are unstable. Out of the remaining clear solultions, many involve doubly-bonded oxygen which quenches scintillation.

Still, the results of the analytical expressions derived in this document are encouraging. We enthusiastically await the results of Monte Carlo simulations which will determine what energy resolution is necessary to observe the $\beta\beta(0\nu)$ peak of ^{100}Mo. Armed with these analytical equations, the appropriate dimensions and design for a detector can be quickly and effectively evaluated once the desired energy resolution is known.

[4] PerkinElmer Optoelectronics, available at http://opto.perkinelmer.com/Downloads/c30902e.pdf

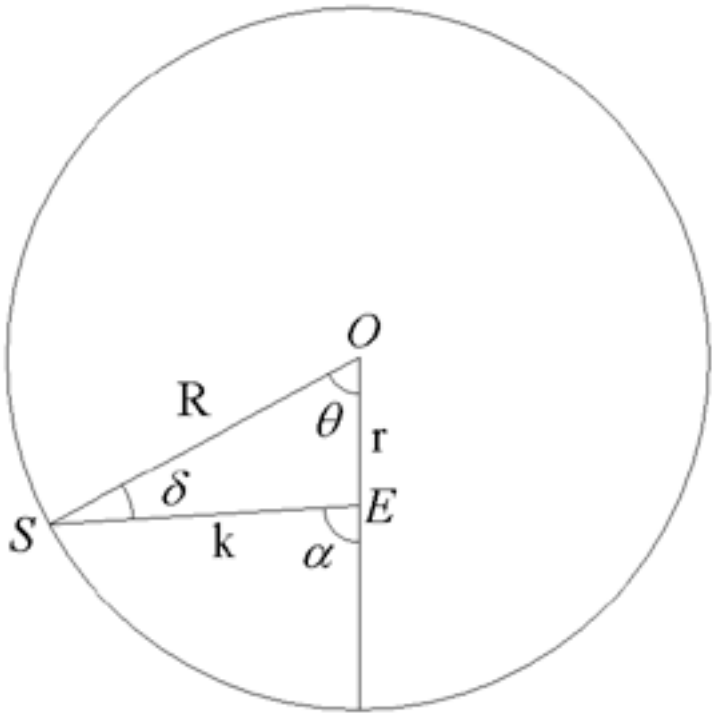

Figure 1: **The Detector Geometry**. An event ocurs at point E. An arbitrary pixel on the surface of the detector sphere is a distance k away from the event, and makes an angle α with the event axis $\overline{OE}$.

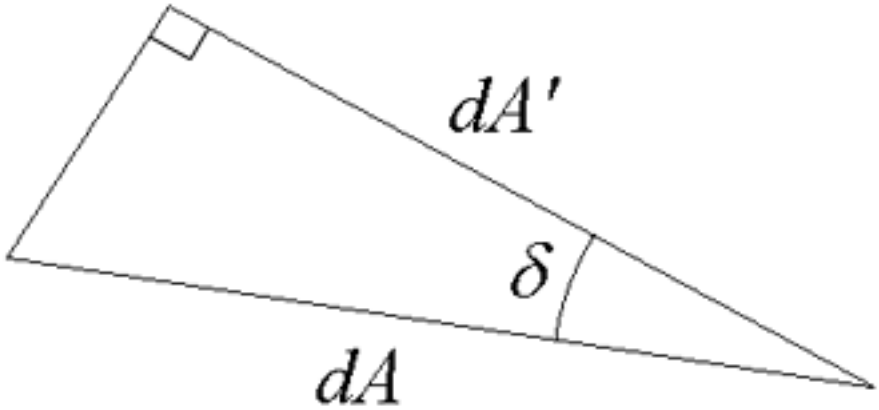

Figure 2: **The area relationship between dA' and dA.** dA' is the area through which the photon flux is $\frac{N}{4\pi k^2}$. The area dA mapped out on the surface of the sphere sees a smaller photon flux by a factor of $\cos(\delta)$.

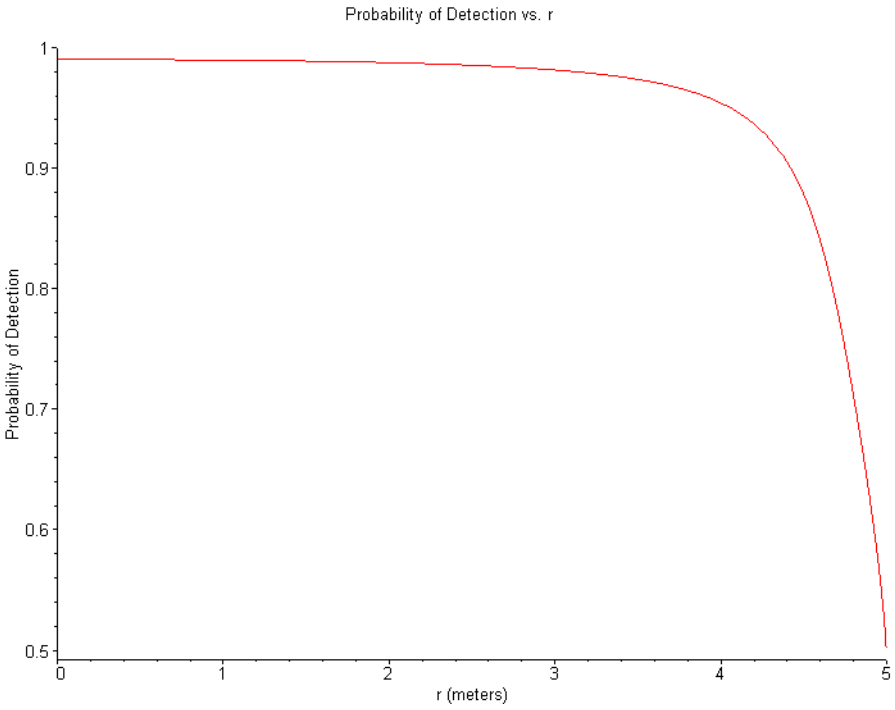

Figure 3: **Probability as a function of** r. The probability of detection p decreases as the event gets closer to the edge of the sphere, because the probability that a pixel is hit by multiple photons increases.

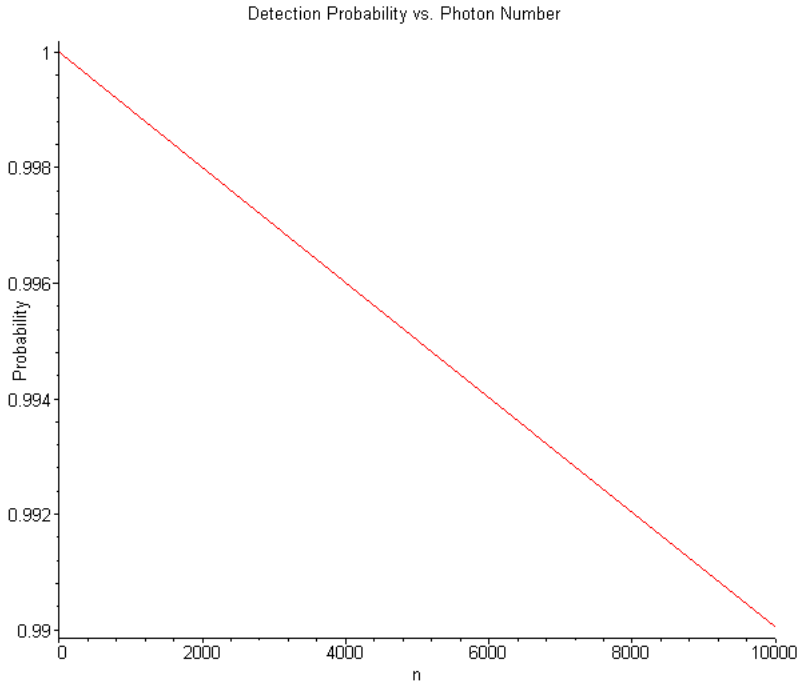

Figure 4: **Probability of Detection as a function of** n. As this graph shows, the probability for detection decreases fairly linearly as the number of previous photons n increases. Thus, we can use the value at $\frac{N}{2}$ to approximate the average probability for each photon in an event of N photons.

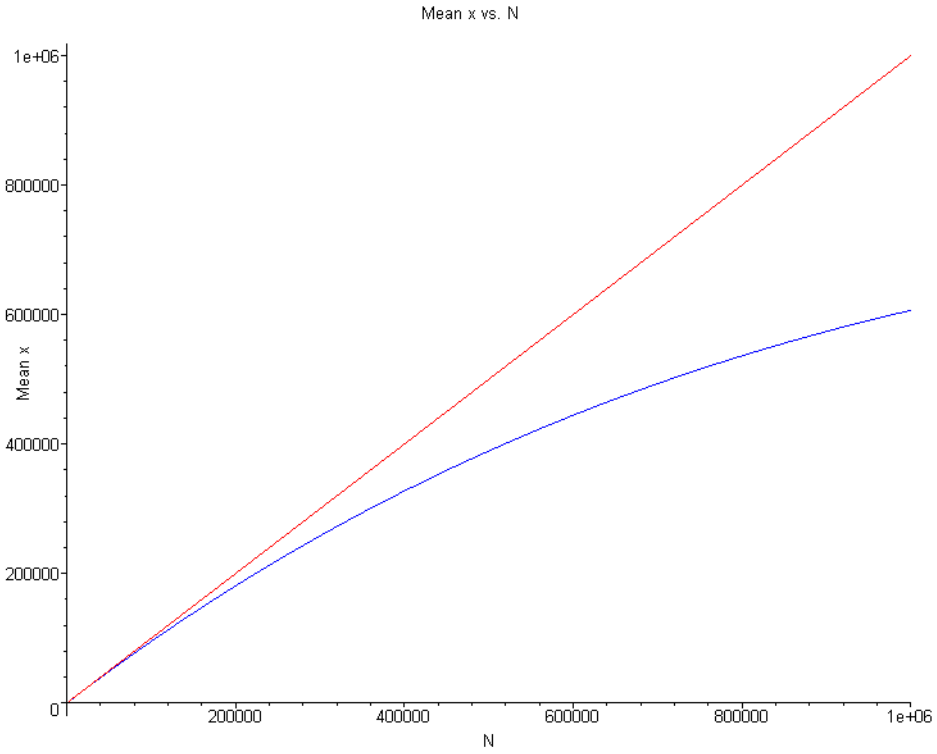

Figure 5: **Mean Number of Hits vs.** N. The mean number of hits seen by the detector varies with the number of source photons N. The slope of this graph is the differential coefficient α which relates number of hits to number of detected photons for a particular value of N.

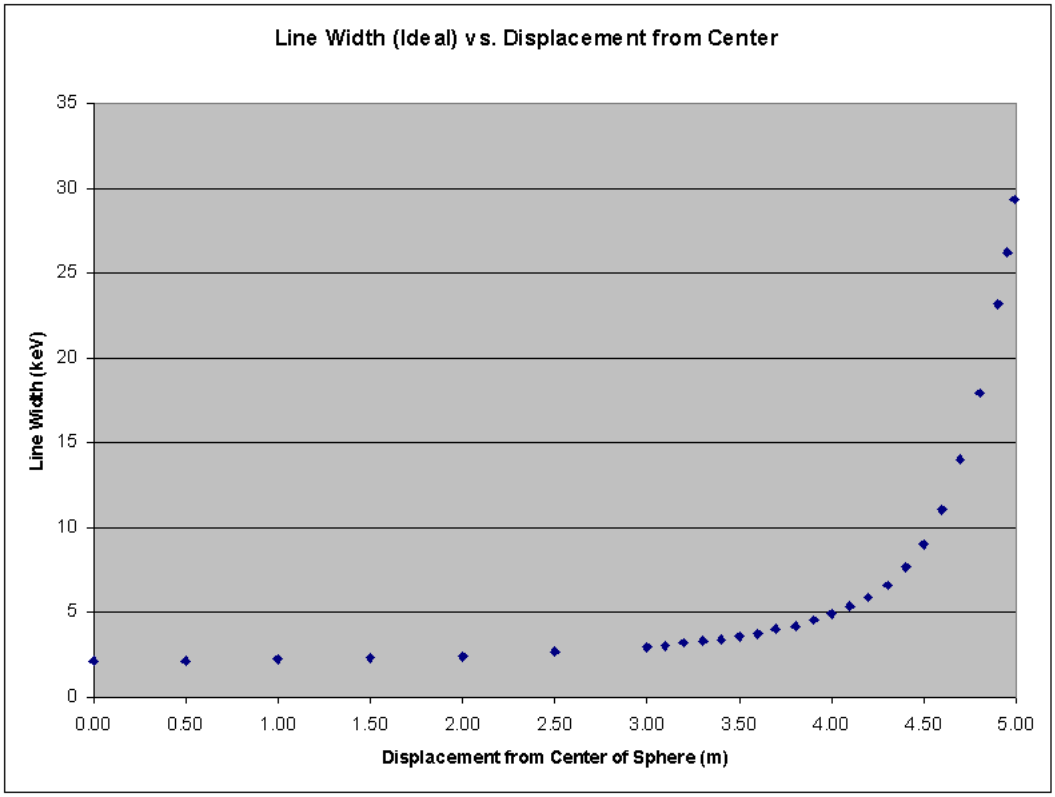

Figure 6: **Line Width as a function of** r. As the event gets closer to the edge, the line width of the energy distribution gets larger, and energy resolution subsequently gets worse. This graph shows that in an ideal situation, the detector proposed would have less that 0.1% energy resolution for events as far off-center as 3m, and better than 0.5% as far out as 4.7m off-center.

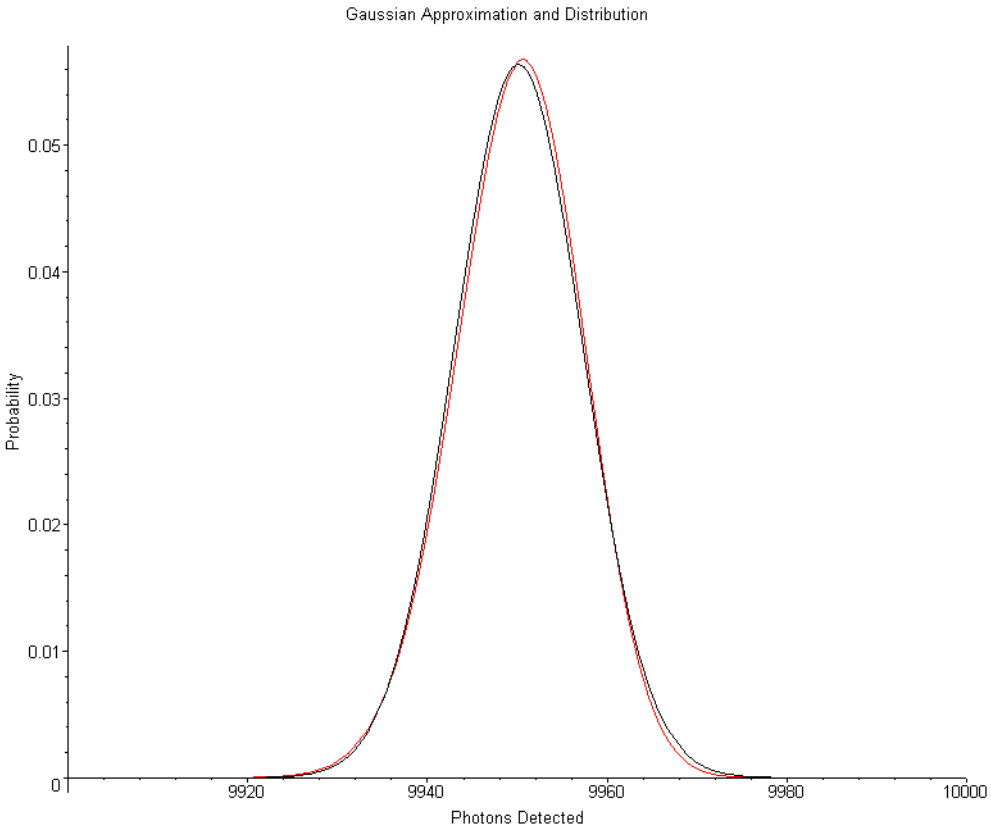

Figure 7: **Probability Distribution and Gaussian Approximation**. This shows the probability distribution for the mean number of hits (upper curve), as well as the Gaussian approximation used to model that distribution (lower curve). The approximation permits rapid computer evaluation of the convolution. This plot is for $r = 0$, $R = 5$, $N = 10^4$, $M = 10^6$.

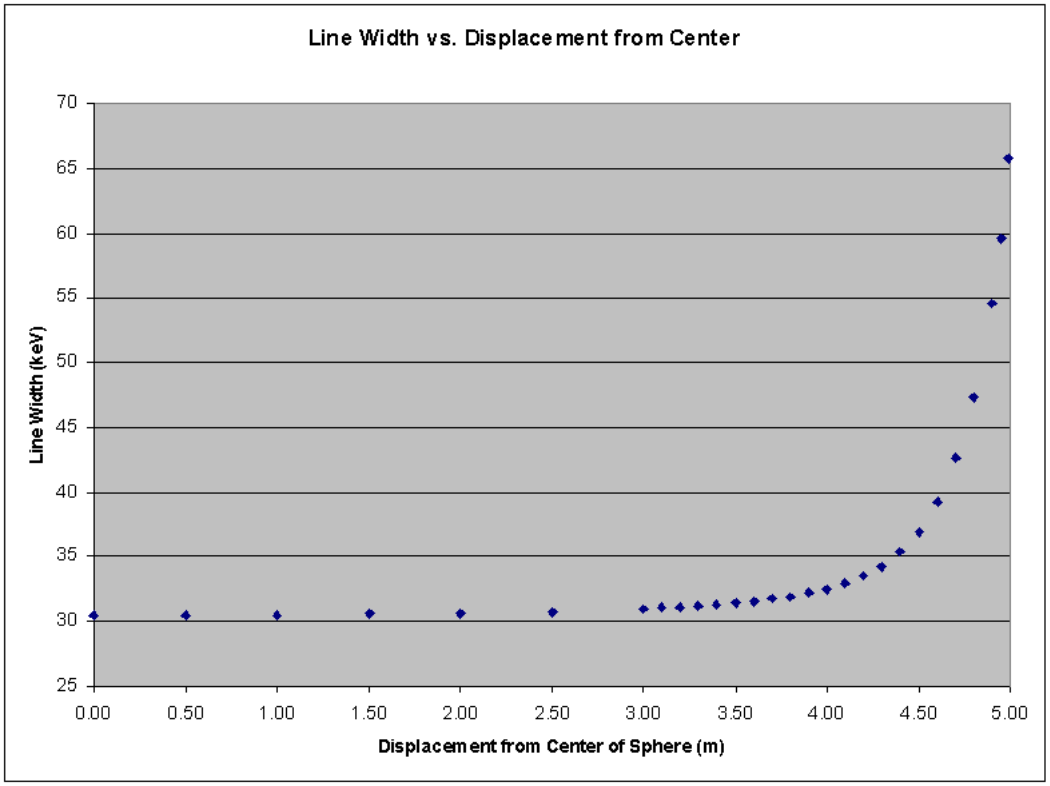

Figure 8: **Line Width as a function of** r. This is a more realistic graph of Line Width vs. r, because it incorporates a source distribution of mean N and standard deviation $\sqrt{N}$. The energy resolution is about 1% as far out as 4m.

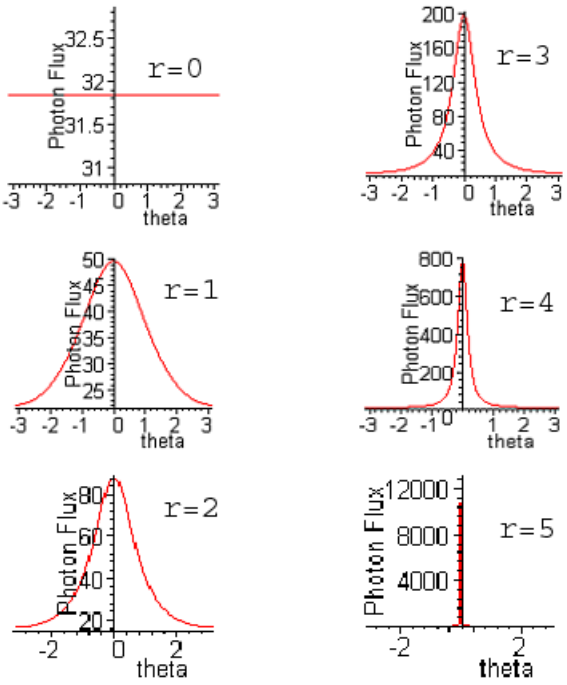

Figure 9: **Photon Flux vs** θ. The hit density of an event as a function of θ should closely resemble the above graphs of Photon Flux vs. θ. If the hit density of an event in the detector is graphed this way, it can be compared to the above graphs to determine the position of the event. Background due to dark counts should be constant in θ, making it possible to subtract out the constant background function from a graph of Hit Density vs. θ. These graphs were generated using equation (8).

Displacement	Line Width (Ideal)		Energy Res	Line Width (More Realistic)		Energy Res
r	(photons)	(keV)*	(percent)	(photons)	(keV)*	(percent)
0.00	7.15120771	2.14536231	0.07151208	101.5997	30.47991000	1.01599700
0.50	7.20032957	2.16009887	0.07200330	101.6269	30.48807051	1.01626902
1.00	7.35405112	2.20621534	0.07354051	101.7127	30.51381432	1.01712714
1.50	7.63362392	2.29008718	0.07633624	101.8714	30.56142423	1.01871414
2.00	8.08324411	2.42497323	0.08083244	102.1336	30.64008480	1.02133616
2.50	8.79033802	2.63710141	0.08790338	102.5630	30.76889442	1.02562981
3.00	9.93901993	2.98170598	0.09939020	103.3043	30.99128895	1.03304297
3.10	10.25243283	3.07572985	0.10252433	103.5042	31.05125280	1.03504176
3.20	10.60479393	3.18143818	0.10604794	103.7495	31.12483602	1.03749453
3.30	11.00317595	3.30095279	0.11003176	104.0326	31.20977418	1.04032581
3.40	11.45648548	3.43694564	0.11456485	104.3624	31.30870911	1.04362364
3.50	11.97609605	3.59282882	0.11976096	104.7505	31.42514742	1.04750491
3.60	12.57677702	3.77303311	0.12576777	105.2127	31.56382185	1.05212740
3.70	13.27803999	3.98341200	0.13278040	105.7708	31.73123037	1.05770768
3.80	14.10616720	4.23185016	0.14106167	106.4549	31.93645758	1.06454859
3.90	15.09737617	4.52921285	0.15097376	107.3082	32.19245412	1.07308180
4.00	16.30286747	4.89086024	0.16302867	108.3936	32.51808294	1.08393610
4.10	17.79726645	5.33917994	0.17797266	109.8050	32.94150609	1.09805020
4.20	19.69288428	5.90786528	0.19692884	111.6864	33.50592648	1.11686422
4.30	22.16503363	6.64951009	0.22165034	114.2640	34.27921449	1.14264048
4.40	25.47373733	7.64212120	0.25473737	117.8823	35.36468067	1.17882269
4.50	30.15650300	9.04695090	0.30156503	123.1903	36.95707935	1.23190265
4.60	36.89316054	11.06794816	0.36893161	130.9603	39.28808103	1.30960270
4.70	46.69514936	14.00854481	0.46695149	142.1720	42.65159757	1.42171992
4.80	59.83177000	17.94953100	0.59831770	157.9311	47.37934008	1.57931134
4.90	77.31181327	23.19354398	0.77311813	181.8626	54.55877850	1.81862595
4.95	87.39284941	26.21785482	0.87392849	198.8478	59.65433679	1.98847789
4.99	97.91007182	29.37302155	0.97910072	219.2611	65.77833345	2.19261112
		* assuming 3Mev/10^4 photons				

Figure 10: **Energy Resolution Data**. This is the data from which the energy resolution graphs were calculated. The line width was determined through a Maple procedure, and then converted to energy (and energy resolution) in Excel, with the assumption that a 3MeV event produces 10^4 photons.